Chapter 4

Charge-Transfer Mutants of the DNA-Bound Glycosylase, Endonuclease III

Abstract:

Endonuclease III (EndoIII) is a base excision repair (BER) glycosylase that targets oxidatively damaged pyrimidines and contains a [4Fe-4S] cluster. We have proposed that the [4Fe-4S] cluster is used in DNA-mediated signaling for DNA repair. Here, several mutants of *E. coli* EndoIII were prepared to probe efficiency of DNA/protein charge transport (CT). Cyclic voltammetry experiments on DNA-modified electrodes show that aromatic residues F30, Y55, Y75, and Y82 help mediate CT between DNA and the [4Fe-4S] cluster in EndoIII. At position 82, an interface between protein and DNA, aromatic residues best facilitate CT, while a serine substitution inhibits protein/DNA CT. Based on circular dichroism studies to measure protein stability, mutations at residues W178 and Y185 are found to destabilize the protein; these residues may function to protect the [4Fe-4S] cluster. These results suggest a pathway for protein/DNA CT and support the model for DNA-mediated signaling between DNA repair proteins as a means of DNA damage detection.

Introduction

First isolated from *Escherichia coli* and described in 1989 [1], Endonuclease III (EndoIII) is an enzyme that excises oxidatively damaged pyrimidines from DNA. EndoIII and MutY, a closely related enzyme that removes adenine mispaired with 8-oxo-7,8-dihydrodeoxyguanine [2, 3], belong to the base excision repair (BER) family of DNA repair proteins, whose members

repair DNA by excising damaged nucleobases from the DNA backbone. EndoIII and MutY homologues are found in many species, ranging from bacteria to humans, and their structural biology and enzymatic properties have been studied in great detail by both crystallography [4–9] and mutagenesis-based enzymology [8, 10–18]. MutY has also drawn attention from the biomedical community because patients with mutations in its human homologue, MUTYH, are predisposed towards developing colorectal cancer [19–23].

Despite these extensive studies, two features of the BER family of enzymes remain intriguing to consider. First, what is the role of the [4Fe-4S] cluster? The [4Fe-4S] cluster does not catalyze base excision in either enzyme, nor is it necessary for MutY to fold properly [11], although it is necessary for MutY to bind DNA. Secondly, how are these proteins able to scan the vast amount of DNA present in a cell in order to detect their substrate lesions? Both enzymes are present in low copy number *in vivo* (~ 30 copies per cell of MutY and ~ 500 copies per cell of EndoIII) [24], making a scan of the genome an unacceptably slow process through a processive mechanism [25].

In response to these questions, our laboratory has proposed a model in which MutY and EndoIII cooperatively scan the genome for DNA lesions using their [4Fe-4S] clusters to participate in DNA-mediated redox signaling [25–28]. DNA mediates CT very efficiently due to π-stacking, or the overlap of aromatic nucleotides whose many delocalized π electrons permit fast electron flow [29–31]. Proteins also mediate CT through a variety of mechanisms [32–37].

These CT mechanisms could permit charge to travel from the DNA into a bound protein, and then through the protein to a redox-active cofactor, such as a [4Fe-4S] cluster.

Both DNA and proteins act as CT mediators in our model for DNA damage detection by DNA-mediated CT. In this model, one protein bound to DNA could transmit an electron through the DNA to a distally bound protein, thus reducing the recipient protein. Reduction decreases the affinity of the protein for DNA [38], so this second protein would dissociate upon reduction and bind to a different location of the genome. However, damaged bases attenuate CT through DNA [39, 40]. Consequently, if DNA between the two proteins is damaged, then charge-transfer is impaired, causing both proteins to remain oxidized and DNA-bound, eventually localizing to the site of damage so that they can repair the lesion. In support of this model, we have found that MutY and EndoIII display physiologically relevant midpoint potentials only when bound to DNA [27, 38]. These protein redox signals are attenuated on electrodes modified with DNA containing an abasic site [27], establishing that the reaction is DNA-mediated. DNA CT can also occur over long distances [29, 41], suggesting that proteins could use it to scan large regions of a genome in order to detect lesions and repair DNA on a reasonable timescale.

One question that remains is how charge is transported from the DNA, through the protein, to the [4Fe-4S] cluster of MutY or EndoIII. Specifically, which amino acids in these proteins facilitate CT between the DNA helix and the

protein metal cluster? One EndoIII mutant, Y82A, has already been shown to be deficient in CT activity, implicating Y82 as a crucial residue in the CT pathway of EndoIII [25]. The current study builds on this result by characterizing several novel mutants of EndoIII to discover other residues that mediate protein-to-DNA CT. Several categories of mutants were prepared, including five additional mutants at or near the Y82 position, to better assess the types of amino acid side chains that are CT proficient in EndoIII. Mutations were also made targeting other aromatic residues in the protein because aromatic amino acids have been shown to mediate CT in other systems [33, 34, 36, 37]. A third category of mutations were made near the [4Fe-4S] cluster, assuming that amino acids close to this redox-active moiety would likely lie along the CT pathway. All of the mutants were characterized by cyclic voltammetry on DNA-modified electrodes, glycosylase assays, and circular dichroism (CD) spectroscopy. These experiments have identified several amino acids that facilitate CT between the DNA helix and the [4Fe-4S] cluster.

Materials and Methods

Preparation of DNA and Protein Samples for Electrochemistry Experiments. Redmond Red (RR) is a redox active probe used to quantify the amount of DNA on the electrode surface [42]. The sequences used for electrochemistry experiments were SH-(C_6H_{12})-(RR)-5'-GA GAT ATA AAG CAC GCA-3' and complement, and SH-(C_6H_{12})-5'-AGT ACA GTC ATC GCG-

3' annealed to 5'-CGC GAT GAC TGT ACT-3'-RR. Redmond-Red was connected to the oligonucleotide via a pyrrolidinyloxy linker. Redmond Red-labeled DNA was prepared according to established methods [41]. Briefly, all DNA sequences were prepared using standard phosphoramidite chemistry on an Applied Biosystems 3400 DNA synthesizer. Phosphoramidites were purchased from Glen Research. For thiolated strands, the 5′ end was modified with the Thiol Modifier C6 S-S phosphoramidite using standard protocols from Glen Research, Inc. DNA modified with Redmond Red on the 3′ terminus was prepared on Epoch Redmond Red CPG columns from Glen Research with ultramild phosphoramidites and reagents. DNA modified with Redmond Red attached to the thiol was prepared with Epoch Redmond Red phosphoramidite from Glen Research with ultramild phosphoramidites and reagents.

Deprotection, purification, chemical modification of DNA, annealing, and preparation of the DNA-modified Au electrode were performed as described previously [43–46]. Au substrates were purchased from Agilent Technologies. Each experiment used 50 μL of 50–100 μM EndoIII in protein buffer (20 mM NaH$_2$PO$_4$ pH 7.5, 100 mM NaCl, 5% glycerol, 1 mM EDTA). The protein concentration was quantified using ε_{410}= 17,000 M^{-1}cm^{-1} [47].

Cyclic Voltammetry. All cyclic voltammetry experiments were performed as described previously [25, 27]. A Au on mica (Molecular Imaging) electrode was assembled and incubated with thiol-modified DNA duplex for 24–36 hours. The electrode was then backfilled with 1 mM mercaptohexanol,

rinsed in DNA buffer (50 mM NaCl, 5 mM NaH_2PO_4 pH 7.5), and then rinsed in protein buffer before protein samples were added to the surface. The DNA-modified Au electrode served as the working electrode, a Pt wire served as the auxiliary electrode, and the reference was either a Ag/AgCl electrode modified with an agarose tip or a 66-EE009 Ag/AgCl reference electrode (ESA Biosciences). All scans were taken at a rate of 50 mV/s on a CH Instruments 760 potentiostat. To determine the relative CT efficiencies of EndoIII mutants, the signal intensity of these proteins was normalized to DNA concentration using the intensity of the Redmond Red signal. For each comparison, the protein samples were measured consecutively on the same electrode surface.

Preparation of EndoIII Over-Expression Construct. The *nth* gene that encodes EndoIII was cloned using the Failsafe Enzyme with Buffer G (Epicentre Biotechnologies) and plasmid pBBR1MCS-4 [48] which contains the *nth* gene as a template. (This construct was originally prepared by cloning the *nth* gene from *Escherichia coli* chromosomal DNA). Primers used were 5'- CGC CCGCG GTGGT ATG AAT AAA GCA AAA GCG CTG– 3' and 5'- CGC GGATCC TCA GAT GTC AAC TTT CTC TTT- 3'. PCR products were purified on a 1% agarose gel and then excised using the QIAquick gel extraction kit (Qiagen). These fragments were ligated into the BamHI and SacII sites of the pET11-ubiquitin-His vector, which expresses hexahistidine and ubiquitin tags at the N-terminus of the insertion site. This vector was derived from the pET11 vector (Novagen), but the ubiquitin gene and hexahistidine tag were engineered into the

vector by the laboratory of Professor Stephen Mayo, from whom this vector was a kind donation. The ligation reaction was used to transform both DH5α *E. coli* (Invitrogen) for sub-cloning, and BL21star(DE3)pLysS *E. coli* (Invitrogen) for over-expression. Transformants resistant to ampicillin and chloramphenicol were selected and the plasmids were isolated using the QIAPrep MiniPrep kit (Qiagen). After the size of the insert was verified by restriction digestion, plasmids from positive transformants were submitted for sequencing (Laragen). Freezer stocks of transformants containing the correct EndoIII sequence were prepared and stored at -80°C.

Purification of EndoIII and Mutants. Freezer stocks of BL21star(DE3)pLysS containing pET11-ubiquitin-His with the *nth* gene were used to inoculate 10 mL of LB media containing 100 μg/mL ampicillin and 30 μg/mL chloramphenicol. Each 10 mL culture was incubated at 37°C overnight and then used to inoculate 1 L of LB/ampicillin/chloramphenicol. Each 1 L flask was grown to OD_{600} = 0.6 at 37°C and then isopropyl β-D-1-thiogalactopyranoside was added to a total concentration of 0.3 mM. Cells were incubated at 30°C for 3.5 hours and harvested by centrifugation (5000 rpm, 10 minutes). Pellets were stored at -80°C. For lysis, pellets were dissolved in 25 mL lysis buffer (50 mM Tris-HCl, pH 8, 5% glycerol, 250 mM NaCl, 5 mM DTT, 1 mM phenylmethylsulfonyl fluoride) and lysed by sonication. Cell lysate was fractionated by centrifugation (7000 rpm, 10 minutes). The supernatant was filtered, and then loaded onto a 5 mL HisTrap HP column (GE Healthcare) pre-

equilibrated with binding buffer (20 mM sodium phosphate, 0.5 M NaCl, 20 mM imidazole, 1 mM DTT, pH 7.4) at a flow rate of ~ 1 mL/min. The column was washed with binding buffer until the UV baseline was stable. The fusion protein was eluted using a gradient of 0–100% elution buffer (20 mM sodium phosphate, 0.5 M NaCl, 500 mM imidazole, 1 mM DTT, pH 7.4) over 10–20 column volumes on an AKTA FPLC (GE Healthcare). Fractions containing protein (determined by their yellow color) were pooled and loaded onto a Superose 12 column (GE Healthcare) that had been pre-equilibrated with Superose 12 Buffer (50 mM NaH_2PO_4, 0.15 M NaCl, pH 7.0). The tagged EndoIII, His_6-ubiquitin-EndoIII, eluted after ~ 12 mL. Fractions containing EndoIII were pooled and dialyzed overnight into protein storage buffer (20 mM sodium phosphate pH 7.5, 0.5 mM EDTA, 100 mM NaCl, 20% glycerol). Aliquots of 50–70 μL EndoIII were prepared, frozen in dry ice, and stored at -80°C. Protein purity was assessed by SDS-PAGE, and concentration was measured using $\varepsilon_{410}= 17,000$ $M^{-1}cm^{-1}$ [47].

Site-Directed Mutagenesis. Mutations were encoded on the pET-11 based EndoIII overexpression plasmid using the Quikchange Site-Directed Mutagenesis Kit (Stratagene). Primers used are listed in the supporting material, where uppercase letters indicate the encoded mutation. DNA primers were purchased from Integrated DNA Technologies. All mutagenized plasmids were sequenced (Laragen) to verify accurate mutagenesis before being used for protein over-expression.

Instrumentation. All protein samples were examined using a Beckman DU 7400 spectrophotometer. Protein concentration was measured using ε_{410} = 17,000 M^{-1}cm^{-1} [47].

Circular Dichroism. Samples were measured at a concentration of ~ 5 μM at ambient temperature on a Model 62A DS Circular Dichroism Spectrometer (AVIV, Lakewood, NJ). For thermal denaturation experiments, the temperature was varied from 20°C to 60°C. Each trace shown is the average of at least three independent experiments.

DNA Glycosylase Assay. This protocol was adapted from methods described previously [10]. DNA strands synthesized were 5'- TGT CAA TAG CAA GXG GAG AAG TCA ATC GTG AGT CT- 3' where X = 5-hydroxyuracil and the complement with G opposite X. DNA was prepared using standard phosphoramidite chemistry using reagents purchased from Glen Research. Prior to annealing, single-strand DNA was purified using reversed-phased HPLC and the substrate-containing strand was 5'- radiolabeled using ^{32}P-ATP [49] with polynucleotide kinase purchased from Roche.

Glycosylase activity was determined by monitoring nick formation in the hydroxyuracil-containing duplex using denaturing gel electrophoresis [12]. For this assay, 100 nM radiolabeled duplex was incubated with EndoIII or a variant at a range of concentrations (10 nM, 100 nM or 1 μM) in reaction buffer (10 mM Tris pH = 7.6, 1 mM EDTA, 50 mM NaCl) for 15 minutes at 37°C. The reactions were quenched upon addition of NaOH to a final concentration of 100 nM.

Samples were dried, counted by scintillation, and diluted with loading buffer (80% formamide, 10 mM NaOH, 0.025% xylene cyanol, 0.025% bromophenol blue in Tris-Borate-EDTA buffer) to normalize the radioactivity. Samples were then heated at 90°C for five minutes prior to loading and then separated by denaturing PAGE. Glycosylase activity was determined by quantifying the amount of 14-mer product visualized in the gel relative to the total amount of DNA present.

Results

Electrochemistry on DNA-modified electrodes. The CT capabilities of several mutants of EndoIII were investigated on a DNA-modified electrode surface passivated with mercaptohexanol (Figure 4.1a). This strategy has been used previously to measure the DNA-bound electrochemical properties of proteins containing [4Fe-4S] clusters [25, 27]. In this study, the thiolated DNA duplex was also modified with Redmond Red, a redox probe whose signal intensity can be used to measure the amount of DNA on a given electrode surface [42]. The Redmond Red was positioned so that it could contact the Au surface and be directly reduced without requiring DNA-mediated reduction.

For each EndoIII sample, the electrochemical signal grew in over 30–45 minutes. Scan rate dependence measurements showed a linear relationship between the peak current of the protein and the square root of scan rate, indicative of a diffusion-limited process [50]. These same experiments showed a linear

relationship between the peak current of Redmond Red and scan rate, indicative of a surface-bound species. Figures 4.1b and 4.1c show typical cyclic voltammograms, with two peaks evident, one from the [4Fe-4S] cluter of the DNA-bound protein and one from the Redmond Red probe. When compared on these surfaces, all mutants exhibited midpoint potentials of roughly 80 (±30) mV versus NHE, and all were within error of that of WT (Table 4.1). While the DNA-bound potential for these mutants was seen to be invariant, significant variations in redox signal intensity were observed (Table 4.1 and Figure 4.1d). The signal strength of each mutant was quantified and normalized based on the amount of DNA present on the electrode. To compare the signal strength of each mutant relative to that of the WT, these signals were further normalized by the Redmond-Red-corrected signal strength of WT EndoIII measured on the same surface.

Among the first samples to be examined in this fashion were mutants relevant to colorectal cancer research, those at positions L81 and Y82. Y82F and Y82W exhibit signal strengths within error of that of WT, suggesting that other aromatic residues at position 82 confer CT capabilities equivalent to those of the native tyrosine. By contrast, Y82S exhibits a very weak electrochemical signal relative to WT (Figure 1b, 1d). The signal intensity from Y82C is on average the same as that of WT, although highly variable, possibly due to the ability of cysteine to facilitate electron transfer in certain contexts [32, 51, 52], albeit through the formation of an unstable radical.

After the experiments with Y82 mutants established the importance of aromatic residues for DNA/protein CT, other aromatic amino acids in EndoIII were targeted for mutagenesis studies. F30A, Y55A, Y75A, and H140A were examined. The first three of these mutants all displayed a CT deficiency relative to WT EndoIII (Figure 4.1d). In the protein structure, Y75, Y55, and F30 are relatively close to Y82, and form a line along one side of the protein [5, 7, 9]. These residues may comprise a pathway of aromatic amino acids through which electrons can travel efficiently. Such aromatic "π-ways" have been found in other peptides [36, 37]. The H140A mutant, by contrast, proved CT-proficient in the experiments performed here so no conclusions can be made about its electrochemical properties. However, this residue was found to be enzymatically important (Table 4.2).

The final category of EndoIII mutants examined were W178A and Y185A, substitutions involving aromatic residues close to the [4Fe-4S] cluster. These mutants were expected to produce weak electrochemical signals because of their proximity to the metallocluster, but they instead produced signals that were large and highly variable relative to WT (Figures 4.1c, 4.1d). One explanation for this phenomenon is protein aggregation, as denatured samples can produce large and erratic signals on DNA-modified electrodes (data not shown). However, because the midpoint potentials of these mutants are within error of those produced by other EndoIII samples, it is unlikely that the [4Fe-4S] cluster degraded in W178A and Y185A, given that [3Fe-4S] clusters have different

potentials [53–55] than the [4Fe-4S] cluster. These results with W178A and Y185A prompted further experiments, described below, that suggest these residues may help protect the [4Fe-4S] cluster from exposure to solvent.

Enzymatic assays of mutants' glycosylase activity. The glycosylase activity of each mutant was measured according to established methods [10, 25]. Briefly, 35-mer strands of DNA were synthesized with 5-hydroxyuracil (5-OH-dU), an EndoIII substrate analogue, incorporated into the sequence. The sequence was 5'-radiolabeled with ^{32}P-ATP and annealed to its complement. Solutions of 100 nM DNA were incubated with 1 μM enzyme. Active enzymes will remove 5-OH-dU from the DNA backbone, leaving an abasic site whose phosphodiester bonds are cleaved with 1 M NaOH. This cleavage produces a 14-mer strand, which can be visualized by denaturing PAGE and autoradiography (Figure 4.2). The amount of 14-mer relative to the total quantity of DNA was used to assess enzymatic activity. Mutants that are glycolytically active are able to bind DNA as well as WT. Consequently, this experiment is an important complement to the electrochemical studies, as it verifies that any weak cyclic voltammetry signals produced by mutants stem from a CT deficiency and not an inability to bind DNA.

Of the eleven mutants examined, most were found to exhibit glycosylase activity within error of that of WT EndoIII. The exceptions were F30A and H140A. F30A was slightly impaired in its glycolytic activity, possibly because F30 is located near the substrate binding pocket of EndoIII [5, 7, 9], so mutations

at this position may impede DNA binding. H140A is deficient in glycosylase activity relative to WT (Table 2). In earlier crystallographic studies, the H140 residue was identified as possibly helping EndoIII bind to DNA by providing a positively charged histidine residue that could help coordinate the negatively charged DNA helix [7]. The enzymatic activity results presented here are consistent with that hypothesis.

Circular dichroism to examine the structural stability of EndoIII mutants. While most of the mutants examined gave electrochemical signals with intensities weaker than or within error of those of WT EndoIII, the mutants W178A and Y185A were exceptions to this trend. Consequently, CD experiments were performed to examine the secondary structure of W178A and Y185A. The CD spectra of WT EndoIII and several mutants were examined for both fully folded and thermally denatured protein (Figure 4.3). All folded samples exhibited similar spectral shapes.

In order to examine the stability of W178A and Y185A relative to WT EndoIII, thermal denaturation experiments were performed. In these experiments, the protein sample was heated gradually and its ellipticity was measured as a function of temperature. The ellipticity of all variants measured decreased with increasing temperature, but W178A and Y185A denatured at a lower temperature than WT EndoIII and a CT proficient mutant, Y82F (Figure 4.3). These data indicate that W178A and Y185A are less stable than WT EndoIII.

Discussion

Biochemical characterization of EndoIII Mutants. Eleven mutants of EndoIII were prepared and characterized biochemically in order to identify residues important for protein/DNA CT. They were selected based on several criteria including sequence conservation, aromatic character, and relevance to colorectal cancer research. Additionally, mutations were made in several different regions of the protein to ascertain CT characteristics of different domains. When assayed by cyclic voltammetry on DNA-modified electrodes, all of the mutants display midpoint potentials within error of that of WT EndoIII, indicating an intact [4Fe-4S] cluster, irrespective of the mutation. Thus our focus shifted to monitoring changes in signal intensity as a function of mutation, reflecting differences in coupling along the path for DNA/protein CT. Glycosylase activity was also measured to assay enzymatic activity and, importantly, confirm DNA-binding.

Variations at the protein-DNA interface. L81 and Y82 are both residues whose MUTYH equivalents exhibit mutations in cancer patients [21], and Y82 is well conserved. Additionally, L81 and Y82 are extremely close to the DNA interface in bound EndoIII. This proximity is important when the CT properties of DNA are considered. DNA is able to mediate CT by means of π-stacking, or the overlap of aromatic nucleotides whose many π-bonds provide an efficient conduit for electron flow [28–30, 56–60]. L81 and Y82 may be able to intercalate into the DNA helix [4]. L81 and Y82 would thus join the network of π-bonds in

DNA that facilitate electron flow. Consequently, L81 and Y82 were seen as important residues for mediating CT. Earlier research from our laboratory confirmed this hypothesis by establishing that Y82A is CT deficient relative to WT EndoIII [25]. To follow up on these experiments, additional mutants were made at L81 and Y82 to assess, in more detail, the characteristics of CT-proficient amino acids in EndoIII. L81C is CT-proficient, so no definite conclusions can be made about the electrochemical properties of L81. The mutant Y82S is electrochemically deficient relative to WT EndoIII, whereas Y82F and Y82W are CT proficient, indicating that aromatic amino acids are important mediators of CT at the Y82 position.

Consideration of pathways for DNA-mediated CT. Crystal structures of DNA-bound EndoIII place the [4Fe-4S] cluster and the DNA at roughly 14 Å apart at their closest [5, 7, 9]. At this distance, CT could proceed by either a single-step tunneling process or a multi-step tunneling process, also called hopping, in which amino acids act as "stepping stones" for the electron as it travels through the protein [33, 34, 61–63]. In hopping systems, many of the amino acids through which electrons hop are aromatic residues [34, 61]. With this information in mind, additional mutations were made at aromatic residues closer to the interior of EndoIII to find residues that could be part of a CT pathway. Emphasis was placed on aromatic residues near Y82, as this tyrosine has already been established as CT-active. F30, Y55, and Y75 all display weaker electrochemical signals than WT EndoIII, suggesting they participate in a CT

pathway. The distances covered are 9 Å from Y82 to Y75, 8 Å from Y75 to Y55, and 6 Å from Y55 to F30, which are reasonable distances to consider in the context of hopping [33]. Time-resolved spectroscopy will be necessary to distinguish these pathways. Tunneling efficiency is exponential with distance [62], so even a slight reduction in tunneling distance can increase CT rates significantly.

Beyond F30, the remainder of the CT pathway was not probed for several reasons. First, many residues in the region between F30 and the [4Fe-4S] cluster are part of the helix-hairpin-helix motif of EndoIII, a well-conserved motif in DNA-binding proteins [9, 64] that helps these proteins interact with their substrates. Mutations in this region could render the protein unstable and/or unable to bind DNA. Second, mutations in this region of the protein may not exhibit a detectable CT deficiency even if the targeted residues are able to facilitate CT, because multiple CT pathways could be present, as is often the case in redox-active proteins [63]. In ribonucleotide reductase, for example, electrons are known to find alternative pathways between two redox centers if a primary pathway is impeded by mutagenesis or incorporation of a non-natural amino acid [34, 35]. Similar phenomena could occur in EndoIII, especially given that all of the mutants examined display at least a partial signal, and that the degree of attenuation lessens as the mutations are made further from the DNA. The signal from Y82A is 50 % ± 13 % that of WT [25], whereas the signal from F30A is 88 % ± 3 % that of WT. These values suggest that protein/DNA CT may involve

Y82, but that it could circumvent F30. Third, mutations very close to the [4Fe-4S] cluster could compromise the stability of this cluster, as may have been the case with the mutants W178A and Y185A.

Characterization of EndoIII mutants with large electrochemical signals. After establishing that mutations in aromatic residues are more likely to impede CT in EndoIII, the mutants W178A and Y185A were expected to produce weak cyclic voltammetry signals. However, their CT activity is unexpectedly high, larger even than that of WT EndoIII. This increase in signal strength may be attributed to structural changes near the [4Fe-4S] cluster of the protein. The loss of the bulky, aromatic residues could increase the conformational flexibility of EndoIII, allowing water molecules to access the protein and accelerate CT to the [4Fe-4S] cluster [65, 66].

One question that could be raised by this result is why alanine is not present at positions 178 and 185 in the native protein since it permits more efficient CT than tryptophan and tyrosine at these positions. A possible answer to this question is presented by the circular dichroism data. W178A and Y185A are found to be less stable structurally than WT, and the resulting instability or flexibility could affect the nearby [4Fe-4S] cluster. Aromatic residues could play a protective role as well. If the [4Fe-4S] cluster decomposes, as could happen as a result of oxidative stress [12, 53], then this cluster could degrade to a [3Fe-4S] cluster. Given the proximity of W178 and Y185 to the [4Fe-4S] cluster of EndoIII, it is also possible that these aromatic residues shield the cluster from

solvent exposure under physiological conditions. However, these mutants still exhibit WT level enzymatic activity, indicating that the structural perturbations are probably localized.

Relevance to cancer research. Another noteworthy aspect of this study is the relevance of these EndoIII in the context of colorectal cancer and DNA repair. EndoIII bears structural similarity MUTYH. When MUTYH acquires certain mutations, it is no longer able to repair damage in the adenomatous polyposis coli (APC) gene, which regulates the proliferation of colonic cells [21, 67]. APC is thought to be particularly susceptible to MUTYH activity because it contains 216 "GAA" codons in which a G:C → T:A transversion would result in a stop codon. Genes associated with other cancers do not contain as many such sites [21]. Several MUTYH mutations have been detected in colorectal cancer patients, including those at positions Y114 and Y166 [21]. These residues align with F30 and Y82 in EndoIII, respectively. Since certain mutations at Y82 are deficient in CT activity but not enzymatic activity, perhaps the MUTYH mutants are similarly deficient in CT. According to our BER search model, these mutants would be less effective at detecting DNA damage, allowing mutations to accumulate in the APC gene that could lead to colorectal cancer.

EndoIII mutants and the model of DNA-mediated CT for DNA repair. Previous work in our laboratory has developed a model in which EndoIII and other redox-active DNA-bound proteins use DNA-mediated signaling to search the genome for lesions. Here, this model was further investigated by examining

specific amino acids in EndoIII that could mediate CT between the DNA and the [4Fe-4S] cluster. Four residues are found to be part of this CT pathway (F30, Y55, Y75, and Y82). Of the remaining residues studied, one is found to be important for enzymatic activity (H140) and two are found that contribute to protein stability (W178, Y185). In total, these mutants help demonstrate that EndoIII contains a well protected [4Fe-4S] cluster to which electrons travel from the DNA helix using a series of amino acids. In partially elucidating a pathway through which charge can travel between the DNA and the [4Fe-4S] cluster, these data further support the possibility that DNA-bound proteins communicate *in vivo* by means of DNA-mediated long-range signaling.

Table 4.1: DNA-bound electrochemistry of EndoIII mutants [a]

EndoIII	Midpoint potential (mV vs. NHE)[b]	Mutant / WT Ratio (RR corrected)
WT	78	
F30A	97	0.9 ± 0.03
Y55A	97	0.7 ± 0.1
Y75A	88	0.6 ± 0.2
L81C	84	1.1 ± 0.2
Y82C	92	0.8 ± 0.6
Y82F	91	1.2 ± 0.4
Y82S	91	0.4 ± 0.2
Y82W	92	1.4 ± 0.4
H140A[c]	71	1.0 ± 0.2
W178A	83	3.5 ± 2.3
Y185A	85	2.2 ± 1.2

[a] Experimental conditions are described in materials and methods. Each experiment used 50 μL of 50−100 μM EndoIII in protein buffer (20 mM NaH_2PO_4 pH 7.5, 100 mM NaCl, 5% glycerol, 1 mM EDTA).

[b] Measurements have an uncertainty of ± 30 mV.

[c] This sample was not measured using Redmond-Red-modified DNA, although extra trials were performed to verify the midpoint potential and signal strength ratio that are shown.

Table 4.2: Summary of glycosylase assay results with EndoIII mutants [a]

EndoIII	% Activity relative to WT at 1 μM concentration
F30A	93.7 ± 2.6
Y55A	96.7 ± 1.0
Y75A	99.8 ± 4.0
L81C	99.2 ± 0.6
Y82C	99.2 ± 0.5
Y82F	99.4 ± 1.1
Y82S	99.4 ± 1.6
Y82W	98.1 ± 3.6
H140A	39.1 ± 6.8
W178A	98.2 ± 1.7
Y185A	97.3 ± 0.6

[a] Experimental conditions were as described in materials and methods. Experiments were conducted using 1 μM protein and 100 nM annealed duplex in reaction buffer (10 mM Tris pH = 7.6, 1 mM EDTA, 50 mM NaCl) for 15 minutes at 37°C. The reactions were quenched upon addition of NaOH to a final concentration of 100 nM. Samples were dried, counted by scintillation, and diluted with loading buffer (80% formamide, 10 mM NaOH, 0.025% xylene cyanol, 0.025% bromophenol blue in Tris-Borate-EDTA buffer) to normalize the radioactivity. Samples were then heated at 90°C for five minutes prior to loading and then separated by denaturing PAGE. Glycosylase activity was determined by comparing the amount of 14-mer produced to the total amount of DNA. The glycosylase activity of each mutant as a percentage of WT is shown. Most mutants have activity within error of that of WT.

Table 4.3: Circular dichroism melting temperatures of select EndoIII variants [a]

Sample	T_m (C°)
WT	48 ± 1.8
Y82F	47 ± 0.2
W178A	42 ± 0.3
Y185A	43 ± 0.5

[a] Experimental conditions are described in materials and methods. To obtain melting temperatures, the spectra were fitted to a sigmoidal curve using Origin software, (OriginLab, Northampton, MA) and melting temperatures were obtained from these midpoints.

Table 4.4: EndoIII mutagenesis primers

Mutations are emphasized in bold, capital lettering.

Mutant	Primers
F30A	5'- ccgagcttaatttcagttcgcct**GCT**gaattgctgattgccgtactgc- 3' (forward)
	5'- gcagtacggcaatcagcaattc**AGC**aggcgaactgaaattaagctcgg- 3' (reverse)
Y55A	5'- gcgacggcgaaactc**GCC**ccggtggcgaatacgcctgcagc -3'(forward)
	5'- gctgcaggcgtattcgccaccgg**GGC**gagtttcgccgtcgc –3'(reverse)
Y75A	5'-gaaggggtgaaaacc**GCT**atcaaaacgattgggctttataacagc-3' (forward)
	5'-gctgttataaagcccaatcgttttgat**AGC**ggttttcaccccttc-3' (reverse)
L81C	5'- gggtgaaaacctatatcaaaacgattggg**TGT**tataacagcaaagc- 3' (forward)
	5'- gctttgctgttata**ACA**cccaatcgttttgatataggttttcaccc- 3' (reverse)
Y82C	5'-ggtgaaaacctatatcaaaacgattgggctt**TGT**aacagcaaagc-3' (forward)
	5'-gctttgctgtt**ACA**aagcccaatcgttttgatataggttttcacc-3' (reverse)
Y82F	5'-ggtgaaaacctatatcaaaacgattgggctt**TTT**aacagcaaagc-3' (forward)
	5'-gctttgctgtt**AAA**aagcccaatcgttttgatataggttttcacc-3' (reverse)
Y82S	5'- ggggtgaaaacctatatcaaaacgattgggctt**TCT**aacagcaaagc – 3' (forward)
	5'- gctttgctgttagaaagcccaatcgttttgatataggttttcacccc-3' (reverse)
Y82W	5' - ggggtgaaaacctatatcaaaacgattgggctt**TGG**aacagcaaagc – 3' (forward)
	5'-gctttgctgttccaaagcccaatcgttttgatataggttttcacccc-3' (reverse)
H140A	5'- ccgactattgctgtcgacacg**GCC**attttccgcgtttgtaatcg- 3' (forward)
	5'- cgattacaaacgcggaaaat**GGC**cgtgtcgacagcaatagtcgg- 3' (reverse)
W178A	5'-gtcgactgccaccat**GCG**ttgatcctgcacgggcg-3' (forward)
	5'- cgcccgtgcaggatcaa**CGC**atggtggcagtcgac- 3' (reverse)
Y185A	5'-cctgcacgggcgt**GCT**acctgcattgcccgcaagccccgc-3' (forward)
	5'-gcggggcttgcgggcaatgcaggt**AGC**acgcccgtgcagg-3' (reverse)

Figure 4.1: Quantitative cyclic voltammetry of EndoIII variants on DNA-modified electrodes. A) Schematic of DNA-modified electrochemistry. A Au surface is treated with thiol-modified DNA and then backfilled with mercaptohexanol. The covalent Redmond Red redox probe, shown as a red oval, is used to quantify the amount of DNA on the surface. Each protein mutant was allowed to bind DNA on such a surface, and the [4Fe-4S] cluster was measured by cyclic voltammetry. The protein was then rinsed from surface and WT was measured on the same surface. B) Representative cyclic voltammogram of Y82S (brown) compared to WT EndoIII (blue). Y82S exhibits a weaker electrochemical signal. For reference, a scan taken in the absence of protein (buffer only) is also shown (gray). C) Representative cyclic voltammogram of W178A (orange) compared to WT EndoIII (blue) and a buffer-only scan (gray). D) The CT capability of each mutant was quantified based on the area under its redox peak. Each mutant's signal intensity was normalized to the intensity of the signal for WT measured on the same surface.
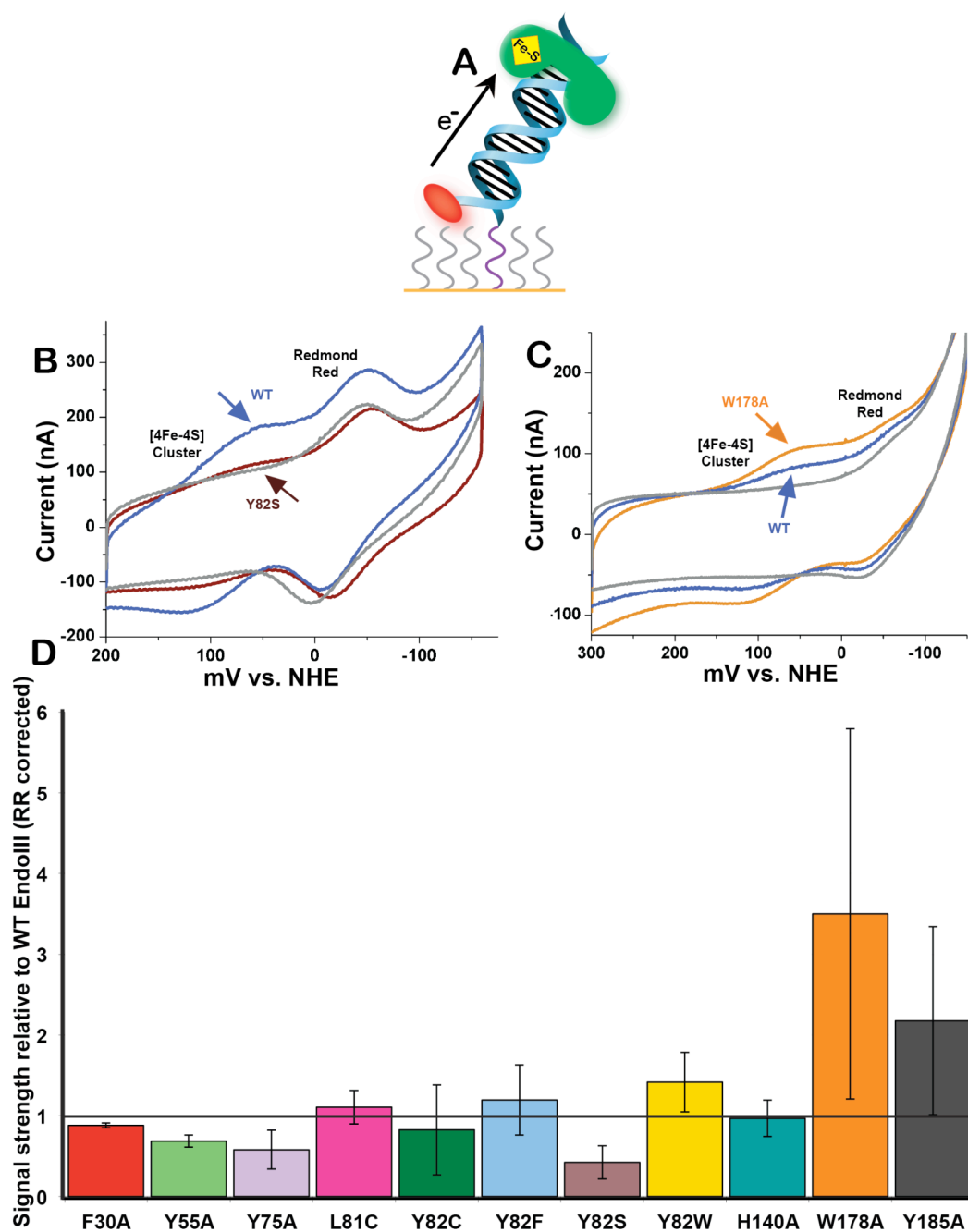
Figure 4.2: Glycosylase assay results of EndoIII variants. For this assay, a 1 μM, 100 nM, or 10 nM protein sample was incubated with 100 nM of 5'-radiolabeled 35-mer duplex DNA containing 5-hydroxy-uracil. Reactions were incubated for 15 minutes at 37°C and quenched with 1 M NaOH. Reactions were then examined by denaturing gel electrophoresis. Cleavage of the DNA results in a 14-mer. The representative gel below shows the results of WT EndoIII (blue) compared to Y75A (purple) and Y185A (black). Enzyme-free control reactions were loaded into the final two lanes. The reactions with 1 μM protein were used to compare the glycosylase activities of EndoIII variants (Table 4.2).
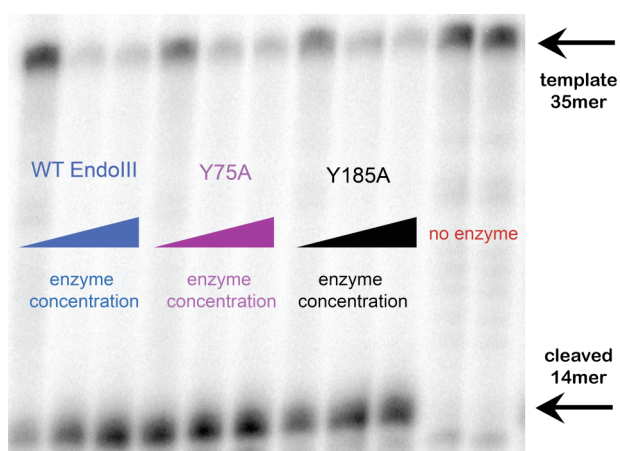
Figure 4.3: Circular dichroism spectra of EndoIII.   A) Comparison of fully folded and denatured spectra of EndoIII.   Samples were measured at room temperature at a concentration of ~ 5 µM. WT spectra are shown, although all mutants displayed a similar trend with denatured samples (gray) consistently displaying less ellipticity than fully folded samples (blue). The spectra shown are the average of three trials.   B) Circular dichroism thermal denaturation of select EndoIII variants. Samples were measured at concentrations of ~ 5 µM. Each spectrum shown is the average of at least three independent experiments.   The spectra show the fractional change in ellipticity for each variant measured, where the fully folded protein was given a value of 0 and the denatured form was given a value of 1, consistent with previous secondary structure studies [11]. The variants WT (dark blue) and Y82F (pale blue) display more structural stability than W178A (orange) and Y185A (black).
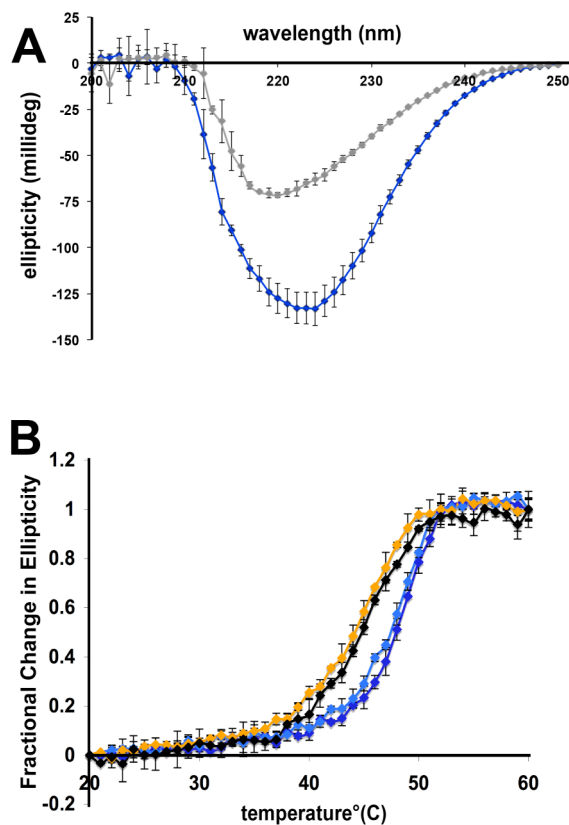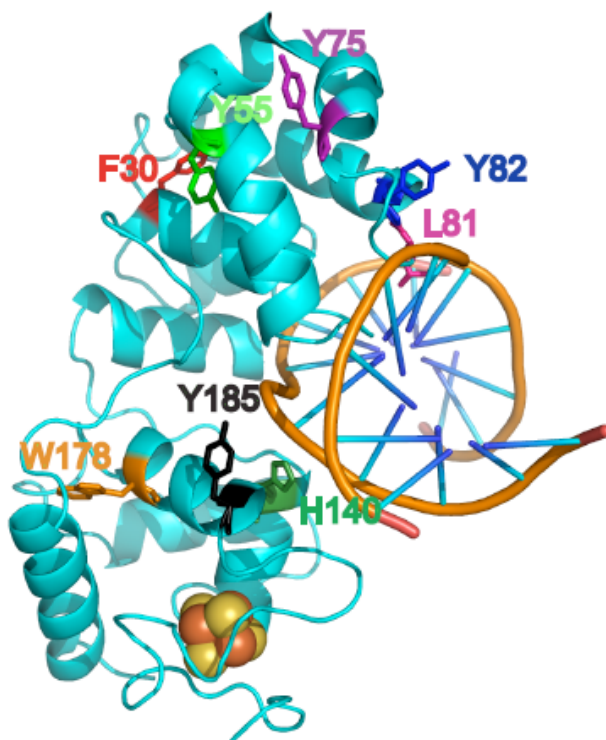
Figure 4.4: Crystal structure of DNA-bound EndoIII. Crystal structure was adapted from references [5, 9] and formatted using PyMol [69]. Residues targeted for mutagenesis studies are emphasized in color.

References:

1. Asahara, H., et al., *Purification and Characterization of Escherichia-Coli Endonuclease-III from the Cloned nth Gene*. Biochemistry, 1989. **28**(10): 4444–4449.

2. Nghiem, Y., et al., *The Muty Gene—a Mutator Locus in Escherichia-Coli That Generates G.C→T.A Transversions*. Proceedings of the National Academy of Sciences of the United States of America, 1988. **85**(8): 2709–2713.

3. Michaels, M.L., et al., *A Repair System for 8-Oxo-7,8-Dihydrodeoxyguanine*. Biochemistry, 1992. **31**(45): 10964–10968.

4. Fromme, J.C., et al., *Structural basis for removal of adenine mispaired with 8-oxoguanine by MutY adenine DNA glycosylase*. Nature, 2004. **427**:652–656.

5. Fromme, J.C., and G.L. Verdine, *Structure of a trapped endonuclease III-DNA covalent intermediate*. The EMBO Journal, 2003. **22**(13):3461–3471.

6. Guan, Y., et al., *MutY catalytic core, mutant and bound adenine structures define specificity for DNA repair enzyme superfamily*. Nature Structural Biology, 1998. **5**:1058–1064.

7. Kuo, C.-F., et al., *Atomic Structure of the DNA Repair [4Fe-4S] Enzyme Endonuclease III*. Science, 1992. **258**(5081):434–440.

8. Manuel, R.C., et al., *Reaction Intermediates in the Catalytic Mechanism of Escherichia coli MutY DNA Glycosylase*. Journal of Biological Chemistry, 2004. **279**: 46930–46939.

9. Thayer, M.M., et al., *Novel DNA binding motifs in the DNA repair enzyme endonuclease III crystal structure*. The EMBO Journal, 1995. **14**(16): 4108–4120.

10. Watanabe, T., et al., *Engineering Functional Changes in Escherichia coli Endonuclease III Based on Phylogenetic and Structural Analyses*. Journal of Biological Chemistry, 2005. **280**(40): 34378–34384.

11. Porello, S.L., M.J. Cannon, and S.S. David, *A Substrate Recognition Role for the [4Fe-4S]2+ Cluster of the DNA Repair Glycosylase MutY*. Biochemistry, 1998. **37**: 6465–6475.

12. Messick, T.E., et al., *Noncysteinyl Coordination to the [4Fe-4S]$^{2+}$ Cluster of the DNA Repair Adenine Glycosylase MutY Introduced via Site-Directed Mutagenesis. Structural Characterization of an Unusual Histidinyl-Coordinated Cluster*. Biochemistry, 2002. **41**: 3931–3942.

13. Livingston, A.L., et al., *Insight into the Roles of Tyrosine 82 and Glycine 253 in Escherichia coli Adenine Glycoslyase MutY*. Biochemistry, 2005. **44**: 14179–14190.

14. Golinelli, M.-P., N.H. Chmiel, and S.S. David, *Site-Directed Mutagenesis of the Cysteine Ligands to the [4Fe- 4S] Cluster of Escherichia coli MutY*. Biochemistry, 1999. **38**: 6997–7007.

15. Chmiel, N.H., et al., *Efficient recognition of substrates and substrate analogs by the adenine glycosylase MutY requires the C-terminal domain.* Nucleic Acids Research, 2001. **29**: 553–564.

16. Bai, H.B., et al., *Functional characterization of two human MutY homolog (hMYH) missense mutations (R227W and V232F) that lie within the putative hMSH6 binding domain and are associated with hMYH polyposis.* Nucleic Acids Research, 2005. **33**(2): 597–604.

17. Bai, H.B., et al., *Functional characterization of human MutY homolog (hMYH) missense mutation (R231L) that is linked with hMYH-associated polyposis.* Cancer Letters, 2007. **250**(1): 74–81.

18. Chepanoske, C.L., et al., *A Residue in MutY Important for Catalysis Identified by Photocross-Linking and Mass Spectrometry.* Biochemistry, 2004. **43**: 651–662.

19. Chmiel, N.H., A.L. Livingston, and S.S. David, *Insight into the Functional Consequences of Inherited Variants of hMYH Adenine Glycosylase Associated with Colorectal Cancer: Complementation Assays with hMYH Variants and Pre-stead-state Kinetics of the Corresponding Mutated E. Coli Enzymes.* J. Mol. Biol., 2003. **327**: 431–443.

20. Al-Tassan, N., et al., *Inherited variants of MYH associated with somatic G:C → T:A mutations in colorectral tumors.* Nature Genetics, 2002. **30**: 227- 232.

21. Cheadle, J.P., and J.R. Sampson, *MUTYH-associated polyposis⸺From defect in base excision repair to clinical genetic testing.* DNA Repair, 2007. **6**: p. 274- 279.

22. Sampson, J.R., et al., *MutYH (MYH) and colorectal cancer.* Biochemical Society Transactions, 2005. **33**: 679–683.

23. Kundu, S., et al., *Adenine removal activity and bacterial complementation with the human MutY homologue (MUTYH) and Y165C, G382D, P391L and Q324R variants associated with colorectal cancer.* DNA Repair (Amst), 2009. **8**(12):1400–1410.

24. Demple, B., and L. Harrison, *Repair of Oxidative Damage to DNA⸺Enzymology and Biology.* Annual Review of Biochemistry, 1994. **63**: 915–948.

25. Boal, A.K., et al., *Redox signaling between DNA Repair Proteins for efficient lesion detection.* Proc. Natl. Acad. Sci. USA, 2009. **106**(36): 15237–15242.

26. Boal, A.K., *DNA-mediated Charge Transport in DNA Repair*, Thesis in Chemistry. 2008, California Institute of Technology: Pasadena, CA.

27. Boal, A.K., et al., *DNA-Bound Redox Activity of DNA Repair Glycosylases Containing [4Fe- 4S] Clusters.* Biochemistry, 2005. **44**: 8397–8407.

28. Genereux, J.C., A.K. Boal, and J.K. Barton, *DNA-Mediated Charge Transport in Redox Sensing and Signaling.* Journal of the American Chemical Society, 2010. **132**(3): 891–905.

29.   Nunez, M.E., D.B. Hall, and J.K. Barton, *Long-range oxidative damange to DNA: effects of distance and sequence*. Chem. Biol., 1999. **6**: 85–97.

30.   Genereux, J.C., and J.K. Barton, *Mechanisms for DNA Charge Transport*. Chemical Reviews, 2010. **110**(3):1642–1662.

31.   Merino, E.J., A.K. Boal, and J.K. Barton, *Biological contexts for DNA charge transport chemistry*. Current Opinion in Chemical Biology, 2008. **12**(2): 229–237.

32.   Giese, B., et al., *Electron Relay Race in Peptides*. Journal of Organic Chemistry, 2009. **74**(10): 3621–3625.

33.   Shih, C., et al., *Tryptophan-accelerated electron flow through proteins*. Science, 2008. **320**(5884):1760–1762.

34.   Stubbe, J., et al., *Radical Initiation in the Class I Ribonucleotide Reductase: Long- Range Proton- Coupled Electron Transfer?* Chemical Reviews, 2003. **103**(6): 2167–2202.

35.   Chang, M.C., et al., *Site-specific replacement of a conserved tyrosine in ribonucleotide reductase with an aniline amino acid: a mechanistic probe for a redox-active tyrosine*. Journal of the American Chemical Society, 2004. **126**(51):16702–16703.

36.   Giese, B., M. Graber, and M. Cordes, *Electron transfer in peptides and proteins*. Curr. Opin. Chem. Biol., 2008. **12**(6): 755-759.

37.   Cordes, M., et al., *Influence of amino acid side chains on long-distance electron transfer in peptides: Electron hopping via "Stepping Stones"*. Angewandte Chemie—International Edition, 2008. **47**(18): 3461–3463.

38.   Gorodetsky, A.A., A.K. Boal, and J.K. Barton, *Direct Electrochemistry of Endonuclease III in the Presence and Absence of DNA*. J. Am. Chem. Soc., 2006. **128**:12082–12083.

39.   Boal, A.K., and J.K. Barton, *Electrochemical Detection of Lesions in DNA*. Bioconjugate Chem., 2005. **16**: 312–321.

40.   Boon, E.M., et al., *Mutation detection by electrocatalysis at DNA-modified electrodes*. Nature Biotechnology, 2000. **18**: 1096–1100.

41.   Slinker, J.D., et al., *DNA Charge Transport over 34 nm*. Nature Chemistry, 2010. **3**: 230–235.

42.   Buzzeo, M.C., and J.K. Barton, *Redmond Red as a Redox Probe for the DNA-Mediated Detection of Abasic Sites*. Bioconjugate Chemistry, 2008. **19**(11): 2110–2112.

43.   Boon, E.M., et al., *DNA-mediated charge transport for DNA repair*. Proc. Natl. Acad. Sci. USA, 2003. **100**: 12543–12547.

44.   Kelley, S.O., et al., *Single-base mismatch detection based on charge transduction through DNA*. Nucleic Acids Research, 1999. **27**(24): 4830–4837.

45.   Kelley, S.O., et al., *Long-Range Electron Transfer through DNA Films*. Angew. Chem. Int. Ed., 1999. **38**(7): 941–945.

46.   Slinker, J.D., et al., *Multiplexed DNA-Modified Electrodes*. Journal of the American Chemical Society, 2010. **132**(8): 2769–2774.

47. Cunningham, R.P., et al., *Endonuclease III Is an Iron-Sulfur Protein.* Biochemistry, 1989. **28**: 4450–4455.

48. Kovach, M.E., et al., *Four new derivatives of the broad- host- range cloning vector pBBR1MCS carrying different antibiotic- resistance cassettes.* Gene, 1995. **166**: 175–176.

49. Sambrook, J., and D.W. Russell, *Molecular cloning: A Laboratory Manual.* 2001, Cold Spring Harbor, NY: Cold Spring Harbor Laboratory Press.

50. Bard, A.J., and L.R. Faulkner, *Electrochemical Methods: Fundamentals and Applications.* 2001, Hoboken, NJ: John Wiley & Sons, Inc.

51. Wang, M., et al., *Electron Transfer in Peptides with Cysteine and Methionine as Relay Amino Acids.* Angewandte Chemie—International Edition, 2009. **48**(23): 4232–4234.

52. Bhattacharjee, S., et al., *Electron transfer between a tyrosyl radical and a cysteine residue in hemoproteins: Spin trapping analysis.* Journal of the American Chemical Society, 2007. **129**(44): 13493–13501.

53. Camba, R., and F.A. Armstrong, *Investigations of the oxidative disassembly of Fe-S clusters in Clostridium pasteurianum 8Fe ferredoxin using pulsed-protein-film voltammetry.* Biochemistry, 2000. **39**(34): 10587–10598.

54. Beinert, H., *Iron-sulfur proteins: ancient structures, still full of surprises.* Journal of Biological Inorganic Chemistry, 2000. **5**(3): 409–409.

55. Beinert, H., *Iron-Sulfur Clusters: Nature's Modular, Multipurpose Structures.* Science, 1997. **277**: 653–658.

56. Giese, B., *Long-distance electron transfer through DNA.* Annual Review of Biochemistry, 2002. **71**: 51–70.

57. Kelley, S.O., and J.K. Barton, *Electron Transfer Between Bases in Double Helical DNA.* Science, 1999. **283**: 375–381.

58. Kelley, S.O., et al., *Photoinduced Electron Transfer in Ethidium-Modified DNA Duplexes: Dependence on Distance and Base Stacking.* J. Am. Chem. Soci., 1997. **119**(41): 9861–9870.

59. Holmlin, R.E., P.J. Dandliker, and J.K. Barton, *Charge transfer through the DNA base stack.* Angewandte Chemie—International Edition, 1997. **36**(24): 2715–2730.

60. Giese, B., *Electron transfer in DNA.* Current Opinion in Chemical Biology, 2002. **6**(5): 612–618.

61. Gray, H.B., and J.R. Winkler, *Long-range electron transfer.* Proceedings of the National Academy of Sciences of the United States of America, 2005. **102**(10): 3534–3539.

62. Gray, H.B., and J.R. Winkler, *Electron tunneling through proteins.* Q. Rev. Biophys., 2003. **36**(3): 341–72.

63. Onuchic, J.N., et al., *Pathway Analysis of Protein Electron-Transfer Reactions.* Annual Review of Biophysics and Biomolecular Structure, 1992. **21**: 349–377.

64.   Doherty, A.J., L.C. Serpell, and C.P. Ponting, *The helix-hairpin-helix DNA-binding motif: A structural basis for non-sequence-specific recognition of DNA*. Nucleic Acids Research, 1996. **24**(13): p. 2488-2497.

65.   Berghuis, A.M., et al., *Mutation of Tyrosine-67 to Phenylalanine in Cytochrome-C Significantly Alters the Local Heme Environment*. Journal of Molecular Biology, 1994. **235**(4): p. 1326-1341.

66.   Casimiro, D.R., et al., *Electron-Transfer in Ruthenium-Modified Cytochromes-C—Sigma-Tunneling Pathways through Aromatic Residues*. Journal of Physical Chemistry, 1993. **97**(50): p. 13073-13077.

67.   Fearnhead, N.S., M.P. Britton, and W.F. Bodmer, *The ABC of APC*. Human Molecular Genetics, 2001. **10**(7): p. 721-733.

68.   *The PyMOL Molecular Graphics System, Version 1.2r3pre*, Schrödinger, LLC.